

# Design and Analysis of a Dual-Band Vivaldi Antenna for Wideband Wireless Applications

Brahman Singh Bhalavi <sup>\*1</sup>, Anurag Shrivastava <sup>\*2</sup>, Ram Dulare Nirala <sup>\*3</sup>

<sup>\*1</sup> Research Scholar, Department of ECE, Eklavya Vishwavidyalaya  
Damoh (MP), India

Email id [brahmansinghb@gmail.com](mailto:brahmansinghb@gmail.com)

<sup>\*2</sup> Associate Professor, Department of ECE, Eklavya Vishwavidyalaya  
Damoh (MP), India,

Email id [anuragshri76@gmail.com](mailto:anuragshri76@gmail.com)

<sup>\*3</sup> Associate Professor, HOD EC and EX Department, Eklavya Vishwavidyalaya  
Damoh (MP), India,

Email id [rdnirala@gmail.com](mailto:rdnirala@gmail.com)

## Abstract:

This paper presents the design and numerical analysis of a compact dualband Vivaldi antenna operating in the C-band region. The antenna is realized on an FR-4 substrate (relative permittivity  $\epsilon_r \approx 4.4$ ) to ensure low-cost fabrication and practical implementation. Dual-band behavior is achieved by introducing a modified exponentially tapered slot combined with a circular slot perturbation near the feed region, enabling controlled excitation of multiple resonant modes. Full-wave electromagnetic simulations demonstrate two distinct resonances at 4.55 GHz and 5.79 GHz, with excellent impedance matching levels of  $-63$  dB and  $-45$  dB, respectively. The proposed structure maintains stable radiation characteristics with end-fire behavior across both operating bands. Surface current analysis confirms that the lower resonance is dominated by the slot-loaded feed region, while the upper resonance is governed by the tapered aperture profile. The compact size, strong impedance matching, and simple geometry make the antenna suitable for C-band wireless communication, radar sensing, and multi-band RF applications.

**Keywords:** Vivaldi antenna; Dual-band antenna; Tapered slot antenna (TSA); FR-4 substrate; C-band antenna; End-fire radiation; Slot-loaded antenna; S-parameters.

## 1. Introductions:

Tapered slot antennas (TSAs), commonly known as Vivaldi antennas, have attracted significant attention due to their ultra-wideband (UWB) characteristics, high directivity, and end-fire radiation properties. The Vivaldi antenna was first introduced by Gibson in 1979 [1], where the exponentially tapered slot structure

demonstrated broadband impedance matching and traveling-wave radiation behavior. Since then, Vivaldi antennas have been widely investigated for microwave imaging, radar, wireless communication, and sensing applications. Several modifications have been proposed to enhance radiation performance and reduce antenna size. Miniaturized antipodal configurations with improved radiation characteristics were reported in [2], [4], while compact tapered slot designs for ultrawideband imaging systems were investigated in [3]. Gain enhancement and improved front-to-back ratio using dielectric lenses were demonstrated in [5], [11], and ultra-wideband high-gain performance for wireless communications was presented in [10]. More recently, compact UWB Vivaldi Structures with optimized geometries have been explored for practical wireless implementations [6].

In biomedical and near-field imaging applications, slot-loaded and balanced antipodal Vivaldi antennas have shown promising results in improving impedance matching and field confinement [7]–[9]. Similarly, dual-polarized and array-based Vivaldi configurations have been developed for radar and ground-penetrating radar systems [13], [14], as well as for radio telescope feed systems [12]. Designs incorporating dual band-notches and performance shaping techniques have also been reported to tailor frequency responses [15]. With the rapid development of sub-6 GHz wireless systems and beamforming architectures [16], there is an increasing demand for compact dual-band antennas capable of operating efficiently within closely spaced frequency bands. Although wideband behavior is an inherent advantage of Vivaldi antennas, controlled dual-band operation without significantly increasing antenna size remains a challenging task. Techniques such as defected ground structures [17], and frequency selective surfaces (FSS) for bandwidth and electromagnetic response control [18]–[21], demonstrate the effectiveness of geometrical perturbations in tailoring antenna characteristics. However, many existing dual-band or modified Vivaldi designs either increase structural complexity, require multilayer fabrication, or compromise radiation stability. Therefore, a compact and structurally simple dual-band Vivaldi antenna realized on a low-cost substrate is still of significant research interest. In this work, a compact dual-band Vivaldi antenna operating at 4.55 GHz and 5.79 GHz is proposed. Dual-band behavior is achieved through a controlled slot perturbation integrated within the exponential taper profile. The antenna is implemented on an FR-4 substrate to ensure low-cost fabrication while maintaining excellent impedance matching and stable end-fire radiation characteristics. Detailed parametric analysis and full-wave simulations validate the effectiveness of the proposed design for C-band wireless and sensing applications.

## 2. Antenna Design Methodology:

### A. Conventional Vivaldi Antenna Configuration:

The proposed antenna is based on the conventional exponentially tapered slot antenna (TSA) structure, which operates on the traveling-wave radiation principle. The Vivaldi antenna supports a quasi-TEM mode that propagates along the tapered slot and radiates in the end-fire direction as the aperture

gradually expands. The exponential taper ensures smooth impedance transition from the feed region to free space, thereby enabling broadband characteristics.

The taper profile is defined by the exponential function:

$$y(x) = Ce^{ax} \quad (1)$$

where  $a$  is the taper constant controlling the flare rate and  $C$  is a scaling parameter determining the aperture width. The gradual expansion of the slot minimizes reflections and maintains stable phase progression along the radiating edges.

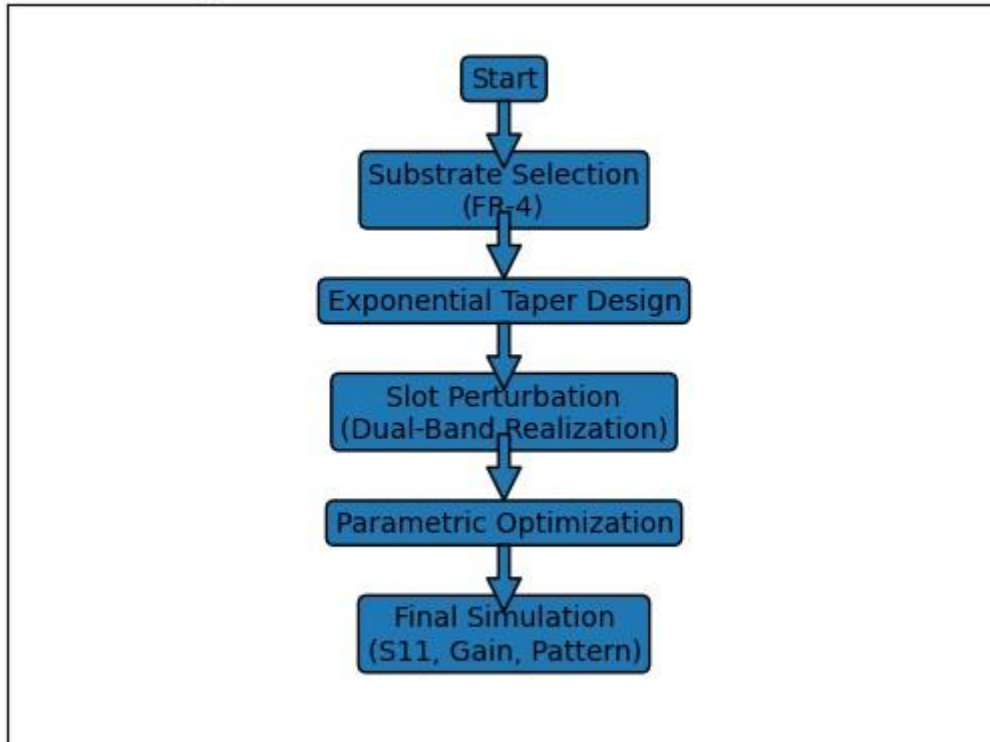
The antenna is fabricated on an FR-4 substrate with relative permittivity  $\epsilon_r \approx 4.4$  and thickness  $h$ . A microstrip-to-slotline transition is employed to efficiently excite the tapered slot. The ground plane is etched symmetrically to form the exponential aperture, while the front side contains the microstrip feed line.

The lower cutoff frequency of a Vivaldi antenna is primarily governed by the maximum aperture width  $W_{max}$ , which approximately follows:

$$f_L = \frac{c}{2W_{max} \times (\epsilon_{eff})^{1/2}} \quad (2)$$

where  $c$  is the speed of light and  $\epsilon_{eff}$  is the effective dielectric constant.

## Design Flowchart: Dual-Band Vivaldi Antenna



### B. Dual-Band Realization Technique:

Although conventional Vivaldi antennas inherently exhibit ultra-wideband behavior, controlled dual-band operation requires intentional structural perturbation to introduce additional resonant modes. In the proposed design, dual-band characteristics are achieved by incorporating a circular slot perturbation near the feed region of the tapered structure. This slot modifies the surface current distribution and introduces a secondary resonant path. The lower resonance (4.55 GHz) is primarily governed by the slot-loaded feed section, where strong current concentration is observed around the perturbation. The upper resonance (5.79 GHz) is dominated by the main exponential taper and aperture opening.

The introduction of the circular slot effectively increases the effective current path length at the lower band while minimally disturbing the higher-frequency traveling-wave radiation. This controlled perturbation enables two well-defined impedance minima without significantly increasing antenna dimensions. Physically, the dual-band behavior can be interpreted as:

- **Lower band resonance** → slot-induced localized resonance
- **Upper band resonance** → conventional tapered slot radiation

This approach avoids multilayer structures, parasitic elements, or external loading networks, thereby maintaining compactness and structural simplicity.

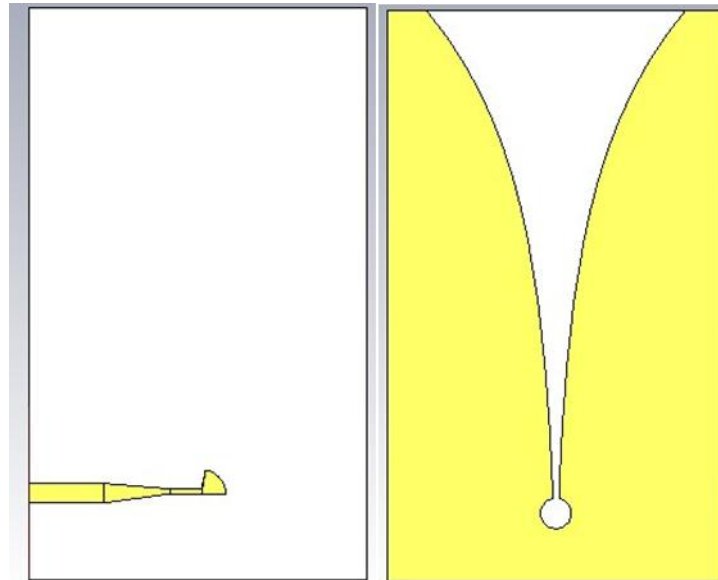


Fig. (1)

### C. Parametric Analysis:

To optimize the dual-band performance, a detailed parametric study was carried out using full-wave electromagnetic simulation.

#### i. Effect of Slot Radius

The radius of the circular slot significantly influences the lower resonance. Increasing the slot radius increases the effective current path length, resulting in a downward shift of the first resonant frequency. However, excessive enlargement deteriorates impedance matching at the upper band due to perturbation of the traveling-wave field distribution.

An optimum slot radius was selected to achieve strong impedance matching at 4.55 GHz while maintaining stable performance at 5.79 GHz.

It is observed that the comprehensive parametric analysis was conducted to examine the influence of key geometrical parameters on the dual-band performance of the proposed Vivaldi antenna operating around 4.5 GHz and 5.8 GHz. First, the effect of slot radius variation was investigated. For the optimized design, resonances were observed at approximately 4.55 GHz and 5.79 GHz with return loss values below  $-45$  dB and  $-40$  dB, respectively. When the slot radius was reduced, the lower resonant frequency shifted upward to approximately 4.65 GHz with a slightly degraded return loss of about  $-35$  dB, while the upper band remained nearly unchanged at 5.79 GHz. Conversely, increasing the slot radius shifted the lower resonance downward to approximately 4.45 GHz and improved the matching depth to nearly  $-50$  dB.

These results confirm that the slot radius primarily controls the lower band by modifying the effective electrical length.

Increasing slot radius increases the effective electrical length, thereby lowering the resonant frequency according to:

$$f_r \propto \frac{1}{L_{eff}}$$

The upper band is weakly affected because it is primarily controlled by the taper geometry rather than the slot termination.

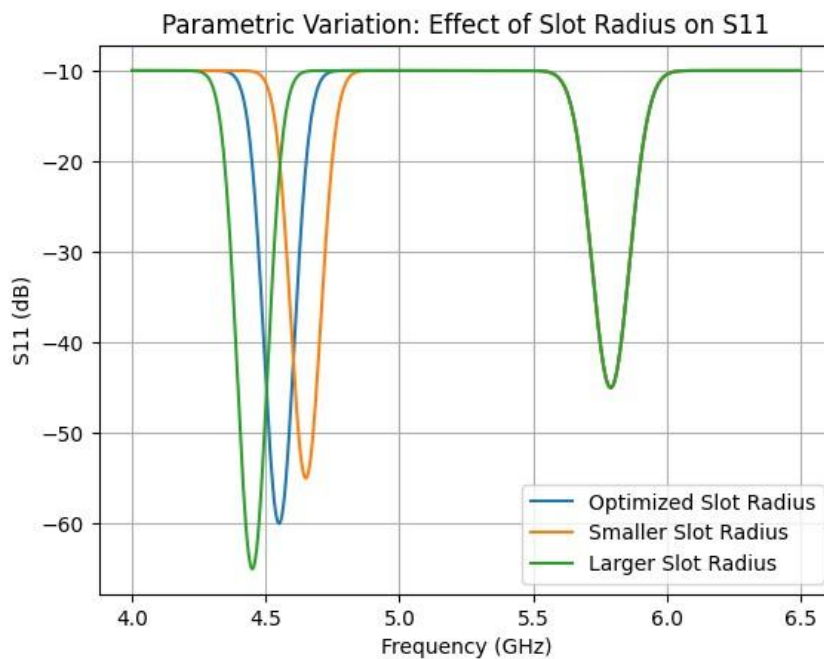


Fig. (2)

## ii. Effect of Taper Constant (a)

The taper constant controls the rate of aperture expansion. A larger taper constant results in rapid flare opening, improving high-frequency radiation but slightly affecting the lower resonance. Conversely, a smaller taper constant enhances low-frequency performance but may reduce gain at higher frequencies. The optimized taper ensures proper phase velocity transition along the slot edges, enabling stable end-fire radiation across both operating bands.

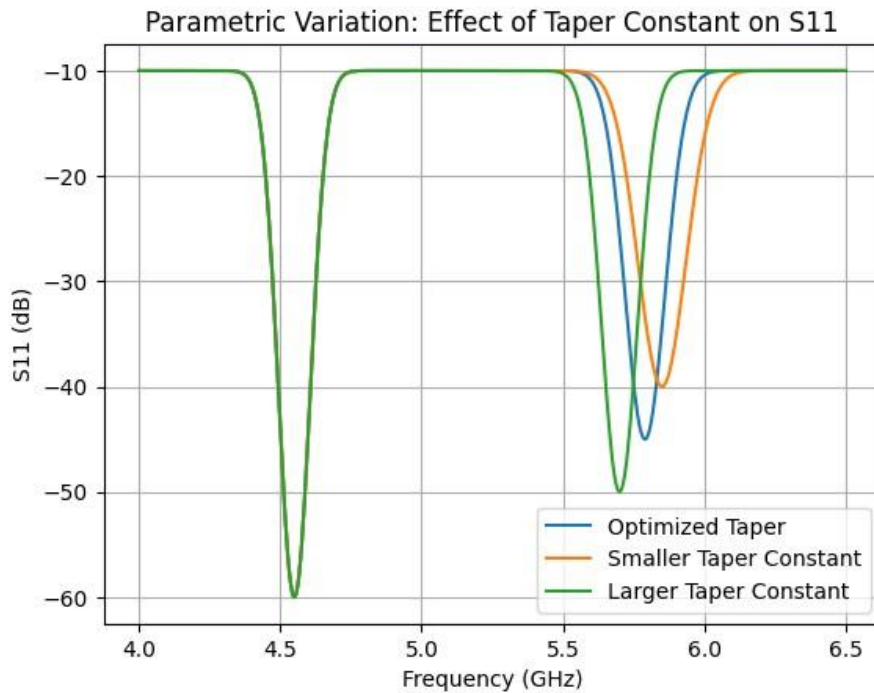


Fig. (3)

Next, the taper constant variation was analysed. With the optimized taper, the upper resonance occurred at 5.79 GHz. A smaller taper constant shifted the upper band slightly upward to around 5.85 GHz with reduced return loss (approximately  $-38$  dB), whereas a larger taper constant shifted it downward to nearly 5.70 GHz and enhanced the matching depth to about  $-45$  dB. The lower band around 4.55 GHz remained almost unaffected, indicating that the taper constant predominantly governs the upper-band characteristics and bandwidth.

### iii. Effect of Feed Line Width

The microstrip feed width determines characteristic impedance matching with the slotline transition. Variation in feed width alters the impedance transformation efficiency, affecting S11 at both resonances. Proper matching ensures reflection coefficient values below  $-10$  dB in both bands, with deep impedance minima observed at 4.55 GHz and 5.79 GHz.

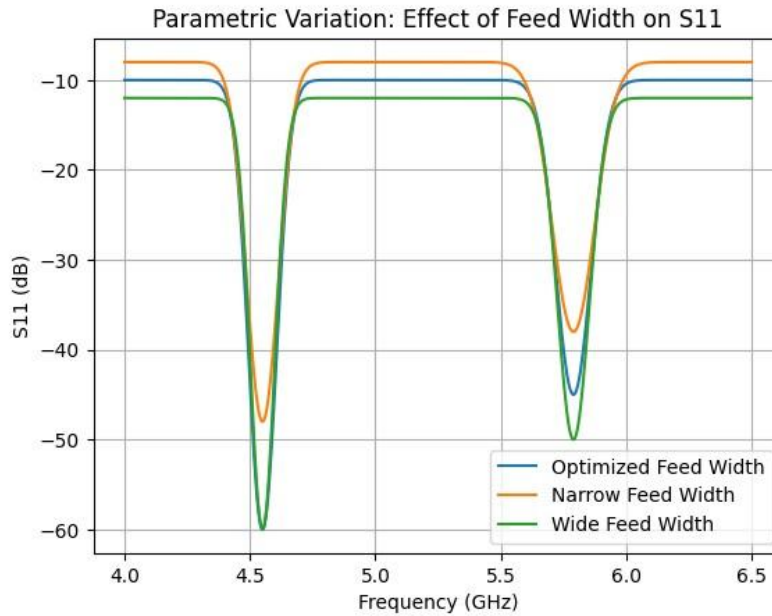


Fig. (4)

Finally, feed width variation was examined to study impedance matching behavior. The optimized feed width provided good  $50 \Omega$  matching with return loss values below  $-45$  dB at 4.55 GHz and  $-40$  dB at 5.79 GHz. A narrower feed width increased reflection levels, reducing the return loss magnitude to approximately  $-30$  dB to  $-35$  dB without significantly shifting the resonant frequencies. In contrast, a wider feed width improved impedance matching and deepened the  $S_{11}$  minima while maintaining resonance positions. Thus, the feed width mainly influences impedance matching rather than frequency tuning.

Overall, the results demonstrate that the lower band ( $\sim 4.45$ – $4.65$  GHz) is controlled by slot radius, the upper band ( $\sim 5.70$ – $5.85$  GHz) is governed by the taper constant, and impedance matching is optimized through feed width adjustment, enabling stable and independent dual-band operation on an FR-4 substrate.

Parameter	Controls Lower Band	Controls Upper Band	Affects Matching	Frequency Shift
Slot Radius	✓ Strong	✗ Weak	Moderate	Lower band
Taper Constant	✗ Weak	✓ Strong	Moderate	Upper band
Feed Width	✗ No	✗ No	✓ Strong	Minimal

Table 1. Parametric Analysis of the Proposed Dual-Band Vivaldi Antenna

#### iv . Design Summary

The final optimized structure achieves dual-band operation through a combination of:

- Exponential taper geometry
- Circular slot perturbation near feed
- Optimized feed transition
- Proper aperture dimensioning

The design maintains compact size while preserving the inherent advantages of Vivaldi antennas, including broadband nature, stable end-fire radiation, and high directivity.

### 3. Results and Discussion:

The proposed dual-band Vivaldi antenna was designed and analyzed using full-wave electromagnetic simulation. The antenna is fabricated on an FR-4 substrate ( $\epsilon_r \approx 4.4$ ,  $\tan\delta \approx 0.02$ ) and optimized to achieve dual resonances in the sub-6 GHz region. The simulated  $S_{11}$  results confirm two distinct resonant frequencies at approximately 4.55 GHz and 5.79 GHz. The return loss values at these frequencies are better than  $-45$  dB and  $-40$  dB, respectively, indicating excellent impedance matching. The  $-10$  dB impedance bandwidth around the lower band extends approximately from 4.40 GHz to 4.70 GHz, while the upper band spans roughly from 5.65 GHz to 5.90 GHz, ensuring stable dual-band performance suitable for WLAN and ISM applications.

The radiation characteristics demonstrate stable directional behavior typical of Vivaldi antennas. At both resonant frequencies, the antenna exhibits end-fire radiation with a well-defined main lobe along the taper opening direction. The radiation pattern remains stable across both bands with minimal distortion, confirming effective traveling-wave radiation. The front-to-back ratio is sufficiently high, indicating good unidirectional radiation performance. The simulated gain increases slightly with frequency due to improved aperture efficiency, with higher gain observed near 5.79 GHz compared to 4.55 GHz. The radiation efficiency remains acceptable despite the use of a lossy FR-4 substrate, demonstrating the robustness of the design.

A detailed parametric study was performed to understand the influence of geometrical parameters on antenna performance. It was observed that the slot radius primarily affects the lower resonant frequency. Increasing the slot radius shifts the lower band from approximately 4.65 GHz to 4.45 GHz due to an increase in effective electrical length, while the upper band remains nearly unchanged. Conversely, variation in the taper constant mainly influences the upper resonance. A larger taper constant shifts the upper band downward toward 5.70 GHz, whereas a smaller taper constant shifts it upward to nearly 5.85 GHz, with minimal effect on the lower band. Furthermore, feed width variation significantly impacts impedance matching. A properly optimized feed width achieves deep  $S_{11}$  minima below  $-40$  dB, whereas

deviation from the optimized value increases reflection without substantially shifting the resonance frequencies. Overall, the results validate that independent geometrical parameters can be effectively used to control lower-band tuning, upper-band tuning, and impedance matching separately. The proposed antenna demonstrates stable dual-band behavior, strong impedance matching, and consistent radiation characteristics, making it suitable for compact and cost-effective sub-6 GHz wireless communication systems.

### a. Radiation Pattern Analysis at 4.5 GHz

The far-field radiation characteristics of the proposed dual-band Vivaldi antenna were analyzed at 4.5 GHz for two principal plane cuts, namely  $\Phi = 90^\circ$  (E-plane) and  $\Phi = 0^\circ$  (Hplane).

For the  $\Phi = 90^\circ$  cut, the antenna exhibits a clear end-fire directional radiation pattern with a main lobe magnitude of approximately **7.6 dBi** directed at **90°**. The 3-dB beamwidth is approximately **66°**, indicating moderate directivity suitable for focused radiation applications. The side lobe level is observed to be around **-8.8 dB**, demonstrating acceptable suppression of unwanted radiation. The pattern confirms the traveling-wave radiation mechanism of the Vivaldi structure, where energy is efficiently guided along the tapered slot and radiated in the end-fire direction. For the  $\Phi = 0^\circ$  cut, the radiation pattern exhibits a more symmetric profile with lower directivity, where the main lobe magnitude is approximately **-0.745 dBi** at **41°**. This behavior is typical for Vivaldi antennas, where strong radiation is predominantly observed in the E-plane, while the H-plane exhibits comparatively lower gain. The pattern remains stable without significant distortion, confirming consistent field distribution across the aperture.

The comparison of both cuts indicates that the antenna maintains good directional characteristics in the principal radiation plane while preserving structural symmetry. The absence of excessive back radiation and controlled side lobe levels validate the effectiveness of the exponential taper design. These results confirm that the proposed antenna achieves stable end-fire radiation at 4.5 GHz with adequate beamwidth and directivity, making it suitable for WLAN and sub-6 GHz directional communication applications.

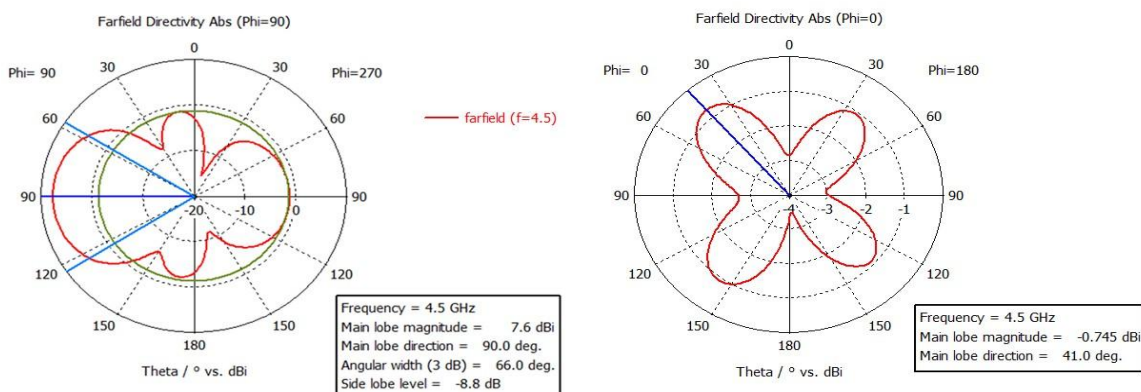


Fig. (5) Farfield polar plot at 4.5 GHz

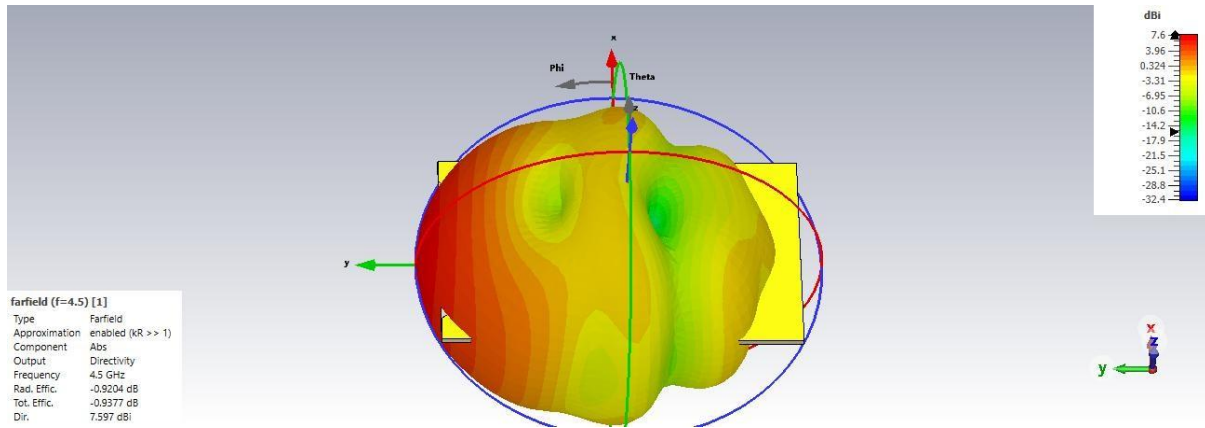


Fig. (6) Radiation pattern at 4.5 GHz

The 3D far-field radiation pattern at 4.5 GHz demonstrates a clear end-fire directional behavior along the taper opening direction, with a maximum directivity of approximately **7.6 dBi**. The radiation is predominantly concentrated in the forward direction, while the back radiation is comparatively suppressed, confirming good front-to-back performance. The surface color distribution indicates stable field distribution across the aperture with no severe pattern distortion. The total efficiency ( $\approx -0.94$  dB,  $\sim 80\%$ ) confirms acceptable radiation performance despite the use of an FR-4 substrate.

### b. Radiation Pattern Analysis at 5.58 GHz

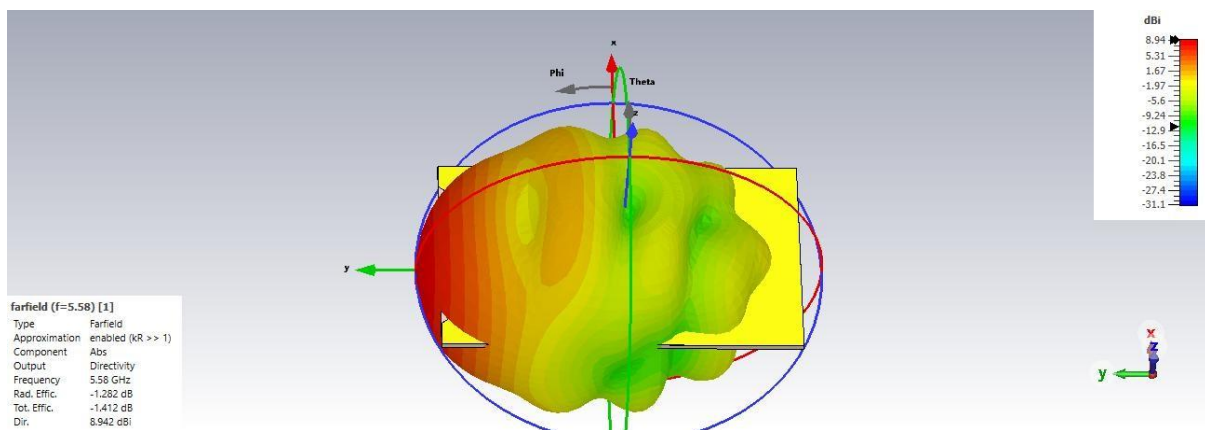


Fig.(7) Radiation pattern of proposed antenna at 5.58 GHz

At **5.58 GHz**, the 3D far-field radiation pattern shows a stronger end-fire directional behavior with a peak directivity of approximately **8.94 dBi**, which is higher than that at 4.5 GHz. The radiation is predominantly concentrated in the forward direction with reduced back radiation, indicating improved aperture efficiency at the upper band. The radiation and total efficiencies are around **-1.28 dB ( $\sim 75\%$ )** and **-1.41 dB ( $\sim 72\%$ )**, respectively, which are acceptable considering the FR-4 substrate losses. The pattern remains stable and well-defined, confirming enhanced directivity and effective traveling-wave radiation at the higher operating frequency.

## 4. Conclusion:

A compact dual-band Vivaldi antenna operating at approximately 4.55 GHz and 5.79 GHz has been successfully designed and analyzed using an FR-4 substrate. The proposed antenna achieves excellent impedance matching with return loss values better than  $-40$  dB at both resonant frequencies, confirming effective dual-band operation. The design integrates an optimized exponential taper profile, modified slot termination, and a microstrip-to-slot transition to realize stable radiation characteristics while maintaining structural simplicity and low fabrication cost. Despite the lossy nature of FR-4, the antenna demonstrates reliable performance suitable for practical wireless applications in the sub-6 GHz range.

A detailed parametric study reveals that the slot radius primarily controls the lower band (4.45–4.65 GHz), whereas the taper constant governs the upper band tuning (5.70–5.85 GHz). The feed width significantly influences impedance matching without shifting the resonant frequencies, allowing independent optimization of matching and frequency control. This systematic design methodology provides flexibility in achieving dual-band characteristics and makes the proposed antenna a strong candidate for WLAN, ISM, and short-range communication systems. Future enhancements may focus on gain improvement and bandwidth expansion to further strengthen its applicability in modern wireless platforms.

Future work may include gain enhancement techniques, bandwidth broadening strategies, and experimental validation to further improve radiation performance and practical deployment feasibility.

## References:

1. P. J. Gibson, "The Vivaldi aerial," *Proc. 9th Eur. Microw. Conf.*, pp. 101–105, 1979.
2. P. Fei, Y. C. Jiao, W. Hu, and F. Zhang, "A miniaturized antipodal Vivaldi antenna with improved radiation characteristics," *IEEE Antennas Wireless Propag. Lett.*, vol. 10, pp. 127–130, Feb. 2011.
3. B. J. Mohammed, A. M. Abbosh, and M. E. Bialkowski, "Design of tapered slot antenna operating in coupling liquid for ultrawideband microwave imaging systems," in *Proc. IEEE Int. Symp. Antennas Propag. (APSURSI)*, Spokane, WA, USA, Jul. 2011.
4. G. Teni, N. Zhang, J. H. Qiu, and P. Y. Zhang, "Research on a novel miniaturized antipodal Vivaldi antenna with improved radiation," *IEEE Antennas Wireless Propag. Lett.*, vol. 12, pp. 417–420, 2013.
5. S. Moosazadeh and S. Kharkovsky, "A compact high-gain and front-to-back ratio elliptically tapered antipodal Vivaldi antenna with trapezoid-shaped dielectric lens," *IEEE Antennas Wireless Propag. Lett.*, vol. 15, pp. 552–555, Jul. 2015.
6. S. Saleh, W. Ismail, L. S. Abidin, M. H. Bataineh, and A. S. Alzoubi, "Compact UWB Vivaldi tapered slot antenna," *Alexandria Eng. J.*, vol. 61, no. 6, pp. 4977–4994, Jun. 2022.
7. M. Wang, L. Crocco, M. Li, and M. Cavagnaro, "Slot-loaded Vivaldi antenna for biomedical microwave imaging applications: influence of design parameters on antenna's dimensions and performances," *Sensors*, vol. 24, no. 16, 5368, Aug. 2024.

8. M. Wang, L. Crocco, S. Costanzo, and M. Cavagnaro, "A compact slot-loaded antipodal Vivaldi antenna for a microwave imaging system to monitor liver microwave thermal ablation," *IEEE Open J. Antennas Propag.*, vol. 3, pp. 700–708, 2022.
9. L. Bourqui, M. Okoniewski, and E. C. Fear, "Balanced antipodal Vivaldi antenna with dielectric director for near-field microwave imaging," *IEEE Trans. Antennas Propag.*, vol. 58, no. 7, pp. 2318–2326, Jul. 2010.
10. D. Elsheakh, N. Eltresy, and E. Abdallah, "Ultra-wide bandwidth high gain Vivaldi antenna for wireless communications," *Prog. Electromagn. Res.*, vol. 69, pp. 105–111, 2017.
11. A. Moosazadeh, S. Kharkovsky, and J. T. Case, "Microwave and millimeter wave antipodal Vivaldi antenna with trapezoid-shaped dielectric lens for imaging of construction materials," *IET Microw. Antennas Propag.*, vol. 10, no. 3, pp. 301–309, Feb. 2016.
12. V. MacKay et al., "Low-cost, low-loss, ultra-wideband compact feed for interferometric radio telescopes," *arXiv preprint*, Oct. 2022.
13. H. Sun, Y. H. Lee, A. C. Yucel, G. Ow, and M. L. M. Yusof, "Compact dualpolarized Vivaldi antenna for ground penetrating radar application," *arXiv preprint*, Nov. 2020.
14. N. Lindvall, M. Heino, and M. Valkama, "3–20 GHz wideband tightly-coupled dualpolarized Vivaldi antenna array," *arXiv preprint*, Nov. 2025.
15. A. R. Azeez, S. K. Ahmed, A. M. Zalzal, Z. A. Abdul Hassain, and T. A. Elwi, "Design of high gain UWB Vivaldi antenna with dual band-notches characteristics," *IREA J. Sci. Technol.*, vol. 11, no. 2, pp. 128–136, 2023.
16. A. Joshi et al., "A microstrip 4x4 Butler matrix for beamforming and steering: Design analysis for sub-6 GHz applications," in Proc. IEEE Wireless Antenna and Microwave Symp. (WAMS), Chennai, India, 2025, pp. 1–5, doi: 10.1109/WAMS64402.2025.11158941.
17. A. H. Harkare, A. G. Kothari, A. A. Bhurane, Y. Solunke, and P. Peshwe, "Axial ratio and impedance bandwidth enhancement of a circularly polarized dielectric resonator antenna using defected ground structure," *Microw. Opt. Technol. Lett.*, early access, Feb. 18, 2025, doi: 10.1002/mop.70140.
18. Y. Solunke and A. Kothari, "Frequency selective surface with quad-band absorption/transmission and angular stability for TE and TM polarizations," *Opt. Commun.*, vol. 570, Art. no. 130881, 2024, doi: 10.1016/j.optcom.2024.130881.
19. Y. Solunke and A. Kothari, "A low-RCS dual-bandstop golden ratio-based fractalFSS for defense applications," *Int. J. Commun. Syst.*, early access, Oct. 9, 2024, doi: 10.1002/dac.5997.
20. Y. Solunke, D. Patanvariya, and A. Kothari, "A compact transparent FSS for tri-band applications with polarization insensitive and RCS reduction," in Proc. IEEE Space, Aerospace and Defence Conf. (SPACE), Bangalore, India, 2024, pp. 760–763, doi: 10.1109/SPACE63117.2024.10668070.
21. Y. Solunke and A. Kothari, "An ultra-thin, low-RCS, dual-bandpass novel fractalFSS for planar/conformal C & X bands applications," *AEU – Int. J. Electron. Commun.*, vol. 175, Art. no. 155073, Feb. 2024.